Diabetes-Induced NF-κB Dysregulation in Skeletal Stem Cells Prevents Resolution of Inflammation

Kang I. Ko,[1] Abby L. Syverson,[1] Richard M. Kralik,[1] Jerry Choi,[1] Brett P. DerGarabedian,[1] Chider Chen,[2] and Dana T. Graves[1]

Diabetes 2019;68:2095–2106 | https://doi.org/10.2337/db19-0496

Type 1 diabetes (T1D) imposes a significant health burden by negatively affecting tissue regeneration during wound healing. The adverse effect of diabetes is attributed to high levels of inflammation, but the cellular mechanisms responsible remain elusive. In this study, we show that intrinsic skeletal stem cells (SSCs), a subset of mesenchymal stem cells, are essential for resolution of inflammation to occur during osseous healing by using genetic approaches to selectively ablate SSCs. T1D caused aberrant nuclear factor-κB (NF-κB) activation in SSCs and substantially enhanced inflammation in vivo. Constitutive or tamoxifen-induced inhibition of NF-κB in SSCs rescued the impact of diabetes on inflammation, SSC expansion, and tissue formation. In contrast, NF-κB inhibition in chondrocytes failed to reverse the effect of T1D. Mechanistically, diabetes caused defective proresolving macrophage (M2) polarization by reducing TGF-β1 expression by SSCs, which was recovered by NF-κB inhibition or exogenous TGF-β1 treatment. These data identify an underlying mechanism for altered healing in T1D and demonstrate that diabetes induces NF-κB hyperactivation in SSCs to disrupt their ability to modulate M2 polarization and resolve inflammation.

Type 1 diabetes (T1D) exerts a detrimental impact on skeletal health by increasing the risk of fractures and causing poor healing (1,2). A striking feature of T1D complications in skeletal injury is a significantly reduced ability to downregulate inflammatory cytokines such as tumor necrosis factor (TNF) (3), which is linked to accelerated cartilage resorption and reduced bone formation (4,5). An anti-inflammatory therapy improves regenerative outcomes in diabetic wounds (4,6), highlighting the importance of limiting inflammation to facilitate healing. While these studies demonstrate the negative impact of chronic inflammation on diabetic healing, little is known about the underlying mechanisms behind the failure to resolve inflammation and maintain homeostasis.

Resolution of inflammation is a critical aspect of tissue regeneration, which is regulated by timely clearance of debris by proinflammatory macrophages and transition toward a phenotype that is proresolving (7). Dysregulated macrophage function leads to excessive tissue destruction and delayed healing (8). Studies have demonstrated that macrophages can regulate the behavior of progenitor cells to maintain homeostasis in bone marrow and the intestinal microenvironment (9,10) and promote regeneration in muscle injury (11). However, a potential reciprocal regulation by stem cells on inflammatory cells during tissue regeneration is poorly understood and remains a fundamental question in the context of immune and stem cell dialog.

A pool of postnatal stem cells resides in the periosteum, endosteum, and stromal compartments in skeletal tissues. In mice, these skeletal stem cells (SSCs) differentiate into chondrocytes and osteoblasts to fully regenerate the lost tissue in response to fracture injury of the long bones (12). Interestingly, expansion of SSCs occurs early in the healing microenvironment (13), suggesting a possible interaction between SSCs and inflammatory cells. SSCs have demonstrated a potent immune-modulatory function in vitro and have been used to treat symptoms of inflammatory diseases (14,15). However, isolation and in vitro expansion of SSCs for transplantation use is artificial and does not accurately represent a potential in vivo function of SSCs. The role of SSCs in regulation of inflammation

[1]Department of Periodontics, School of Dental Medicine, University of Pennsylvania, Philadelphia, PA
[2]Department of Anatomy and Cell Biology, School of Dental Medicine, University of Pennsylvania, Philadelphia, PA
Corresponding author: Dana T. Graves, dtgraves@upenn.edu

Received 18 May 2019 and accepted 9 August 2019

This article contains Supplementary Data online at http://diabetes.diabetesjournals.org/lookup/suppl/doi:10.2337/db19-0496/-/DC1.

in vivo and their potential dysregulation under pathological condition are surprisingly underexplored.

Nuclear factor-κB (NF-κB) is a transcription factor that responds to various stressful stimuli and regulates gene transcription associated with inflammation (16). Aberrant NF-κB activation is observed in podocytes, peripheral neurons, and endothelial and ligament cells in T1D (5,17–19), which is attributed to increased oxidative stress and inflammation that stems from persistent hyperglycemia (20). Pharmacologic inhibition of NF-κB improves vascular function in a diabetic animal model (21), implicating a pathologic role of NF-κB in diabetic complications. While these studies implicate a potential involvement of NF-κB in diabetic bone healing, the precise mechanisms and cell types that control homeostasis remain unknown.

In this study, we report that SSCs play an essential role in modulating inflammation during fracture injury and that T1D interferes with this through aberrant activation of NF-κB. Through genetic manipulation and rescue experiments, we demonstrate that diabetes-induced NF-κB suppresses SSC expansion and production of anti-inflammatory TGF-β1 to cause the failure of macrophage polarization toward a proresolving phenotype. Collectively, our study demonstrates an important reciprocal relationship between immune and stem cell interactions during skeletal regeneration and implicates a potential role of hyperglycemia-induced NF-κB dysregulation in stem cells in other types of injury in which diabetes interferes with the healing process.

RESEARCH DESIGN AND METHODS

Animal Studies

All animal experiments were initiated on 8- to 10-week-old male and female mice conforming to a protocol approved by the University of Pennsylvania Institutional Animal Care and Use Committee. The following mice were purchased from The Jackson Laboratory: C57BL/6J, *B6.Cg-Tg(Prrx1-cre)1Cjt/J* (*Prx1*^{Cre}), *B6.Cg-Tg(Prrx1-cre/ERT2,-EGFP)1Smkm/J* (*Prx1*^{CreER}), *B6.Cg-Gt(ROSA)26Sor*$^{tm9(CAG-tdTomato)Hze}$*/J* (*R26*^{TdTomato}), and *B6.129P2-Gt(ROSA)26Sor*$^{tm1(DTA)Lky}$*/J* (*R26*^{DTA}). *B6;SJL-Tg(Col2α1-cre)1Bhr/J* mice (*Col2α1*^{Cre}) were obtained from Dr. Patrick O'Connor (Rutgers University, Newark, NJ), and floxed *Ikkβ* mice (*Ikkβ*$^{f/f}$) from Dr. Michael Karin (University of California San Diego, La Jolla, CA). Low-dose streptozotocin injection was performed intraperitoneally for T1D induction (5 consecutive days, 50 mg/kg) (Cayman Chemical) as previously described (22). Animals were considered diabetic when blood glucose was >220 mg/dL 1 week after last injection and remained diabetic for 4–6 weeks prior to fracture surgery.

Fracture Induction

A closed-transverse femoral fracture was induced as previously described (4). Briefly, a 27-gauge needle was used to access femoral marrow space via articular cartilage. A 30-gauge pin was inserted into the marrow for wound stabilization. Fracture injury was induced at middiaphysis with controlled weight on a guillotine-like apparatus.

Tamoxifen Injection

Tamoxifen (5 mg/25 g) (Sigma-Aldrich) or corn oil was administered via oral gavage for 5 consecutive days. Fracture injury was induced 24 h after last injection.

Immunofluorescence

Harvested fracture samples were fixed in 10% formalin at 4°C for 24 h, decalcified in 14% EDTA (pH 7.4) for 2 weeks at 4°C with constant agitation, and processed in paraffin or frozen blocks. Immunofluorescence was performed using the following primary antibodies: anti-GFP (NB100-1770; Novus Biologicals), anti-Ki67 (14-5698-82; eBioscience), anti-RFP (600-901-379; Rockland Antibodies), anti–NF-κB (ab16502; Abcam), anti-TNF (ab34674), anti-F4/80 (ab6640), anti-CD4 (ab183685), anti-IKKβ (ab124957), anti-CD271 (ab52987), anti-Sca1 (ab51317), anti–inducible nitric oxide synthase (iNOS) (ab15323), anti-CD163 (ab182422), and anti–TGF-β1 (ab92486). The DeadEnd TUNEL System (G3250; Promega) or Annexin V (A13204; Invitrogen) was used to detect apoptotic cells. Percent-positive cells and mean fluorescence intensity (MFI) were quantified using NIS-Element software (Nikon).

Quantitative RT-PCR

Fracture samples were dissected, snap-frozen in liquid nitrogen, and stored in a −80°C freezer. Samples were pulverized in liquid nitrogen using a prechilled mortar and pestle. RNA isolation (AM1912; Thermo Fisher Scientific) and cDNA preparation (4368813; Thermo Fisher Scientific) were performed following the manufacturer's protocols. Quantitative RT-PCR (RT-qPCR) was performed with Fast SYBR Green (4385614; Thermo Fisher Scientific) on a StepOnePlus System (Applied Biosystems). The primer sequence list is provided in Supplementary Table 2. Data were normalized to housekeeping gene expression (*L32*). In a pilot study, *Tgfb1* had a more pronounced effect than *Il10*; therefore, *Tgfb1* was investigated further.

In Vitro Experiments

Primary bone marrow SSCs (BMSSCs) from female mice were prepared by flushing the femur/tibiae marrow cavity as previously described (14). Briefly, 15×10^6 cells were seeded in 100-mm dishes (Genesee Scientific). Nonadherent cells were removed after initial 24-h incubation in 5% CO_2 at 37°C, and adherent cells were cultured for 14 days in α-minimum essential medium supplemented with 20% FBS, 2 mmol/L L-glutamine (Invitrogen), 55 μmol/L 2-mercaptoethanol (Invitrogen), and 100 units/mL penicillin and 100 μg/mL streptomycin (Invitrogen). For high-glucose experiments, wild-type BMSSCs and BMSSCs with *Ikkβ* deletion were incubated under low-glucose (4.5 mmol/L) or high-glucose (25 mmol/L) conditions in low-serum media containing 2% FBS for 5 consecutive days. TGF-β1 ELISA was performed according to the

manufacturer's protocols (DY1679-05; R&D Systems), including activation of latent TGF-β1.

Bone marrow–derived macrophages (BMMs) were prepared following published protocol (23) using macrophage colony-stimulating factor (20 ng/mL) (315-02; PeproTech). BMMs were stimulated for 24 h with low-dose lipopolysaccharide (LPS) (10 ng/mL) for classically activated macrophage (M1) and IL-4 (1.25 ng/mL) for proresolving macrophage (M2) polarization, in combination with BMSSC-conditioned medium (BMSSC-CM). All conditioned media contained 20% FBS and low glucose (4.5 mmol/L), which were prepared by incubating BMSSCs for 48 h after low- or high-glucose treatment as described above. For TGF-β1–neutralizing experiments, BMMs were stimulated as above with isotype IgG or TGF-β1 antibody (5 μg/mL) (MAD240; R&D Systems) for 24 h.

Recombinant TGF-β1 Treatment

After 24 h postfracture, mice received 100 ng of recombinant TGF-β1 (catalog number 240-B-002; R&D Systems) dissolved in 200 μL of PBS, administered circumferentially around the fracture periosteal layer. Control mice received PBS only.

Statistical Analysis

Statistical analysis was performed using Prism software (GraphPad version 7.03). All data are expressed as the mean ± SD. In vivo experiments comparing multiple groups used two-way ANOVA followed by Tukey post hoc test to determine significance. When comparing two groups, a Student *t* test was performed. In vitro experiments with multiple groups were analyzed with one-way ANOVA. A P value <0.05 was considered statistically significant. Individual animal was used as a unit of measurement, and sex was not considered as a factor in the analyses.

Data and Resource Availability

The data set generated and analyzed in this study is available from the corresponding author upon reasonable request. Research Resource Identifiers for antibodies used in this study are provided in Supplementary Table 1. The resource generated during and/or analyzed during the current study is available from the corresponding author on reasonable request.

RESULTS

To determine if the removal of SSCs has an impact on modulation of inflammation, we selectively ablated SSCs in $Prx1^{CreER\text{-}GFP+}R26^{DTA}$ mice with tamoxifen-induced diphtheria toxin expression driven by an SSC-specific promoter element of *Prx1* (24). Three- and 6-day postfracture time points were selected to examine resolution of inflammation and the early chondrogenesis phase (13), respectively. We followed the loss of SSCs through Prx1-dependent GFP, which is expressed in the fusion protein (Fig. 1*A*). Tamoxifen administration resulted in a significant reduction in GFP^+ SSCs (Fig. 1*B*). SSC ablation led to increased mRNA levels of *Tnf*, *Il1b*, and *Ifng* compared with the control group (Fig. 1*C*), with a corresponding increase in $F4/80^+$ macrophages and $CD4^+$ lymphocytes (Fig. 1*D* and *E*). SSC ablation also led to a significant reduction in cartilage formation, a measure of tissue regeneration, by day 6 (Fig. 1*F*). The number of proinflammatory TNF^+ cells was maintained at high levels through day 6 fractures, when SSCs were removed (Fig. 1*G*). SSC reduction had little effect on basal inflammation in noninjured femurs, as measured by the quantity of $F4/80^+$ and $CD4^+$ cells (Fig. 1*H*) and MFI per cell (data not shown), indicating that SSCs played a primary role in modulating inflammation when there was an inflammatory perturbation stimulated by injury. These data establish that intrinsic SSCs are necessary in limiting inflammation during an early healing response.

A hallmark characteristic of diabetic wound healing is a failure to resolve inflammation (25). Because SSC ablation resulted in elevated inflammation that mirrors diabetic fracture healing, we hypothesized that diabetes-enhanced inflammation is due to its impact on SSCs. We first examined activation of NF-κB by its nuclear localization in normoglycemic and streptozotocin-induced diabetic mice. Immunofluorescence with NF-κB antibody demonstrated that diabetes altered nuclear NF-κB localization in skeletal muscle and periosteum, indicative of its dysregulation, compared with normoglycemic control mice (Fig. 2*A* and *B*). Induction of fracture injury led to the greatest magnitude of NF-κB activation in periosteal cells (Fig. 2*C* and *D*). Given that periosteal cells represent an important SSC population that differentiates into chondrocytes and osteoblasts in vivo (26), we focused our study on the role of NF-κB in SSCs to investigate how its dysregulation affected the diabetic healing process.

We next tested the hypothesis that aberrant NF-κB activation in SSCs is responsible for diabetes-dysregulated inflammation during the early response to fracture healing. We used mice with conditional NF-κB inhibition in SSCs using experimental $Prx1^{Cre+}Ikk\beta^{f/f}$ mice through deletion of floxed *Ikkβ*, an NF-κB activator (27). *Ikkβ* deletion had little to no effect on basal long bone formation, trabeculation, cortical bone area, and weight (Supplementary Fig. 1). $Prx1^+$ SSCs expanded rapidly in the periosteal region 3 days after fracture (Fig. 3*A*). During this period, there was substantial NF-κB activation, as shown by its nuclear localization in the periosteal SSCs and BMSSCs in diabetic wild-type mice, which was accompanied by significantly elevated levels of inflammatory cytokines *Tnf*, *Il1b*, and *Ifng* and reduced levels of anti-inflammatory cytokine *Tgfb1* (Fig. 3*B–D*). The increase in *Tnf*, *Il1b*, and *Ifng* caused by diabetes was completely rescued by inhibition of NF-κB in SSCs alone, and the suppression of *Tgfb1* was reversed (Fig. 3*B–D*). Furthermore, the number of TNF^+ inflammatory cells that was elevated in diabetic wounds returned to normal levels when NF-κB was blocked in SSCs (Fig. 3*E*). A complete reversal of aberrant inflammation

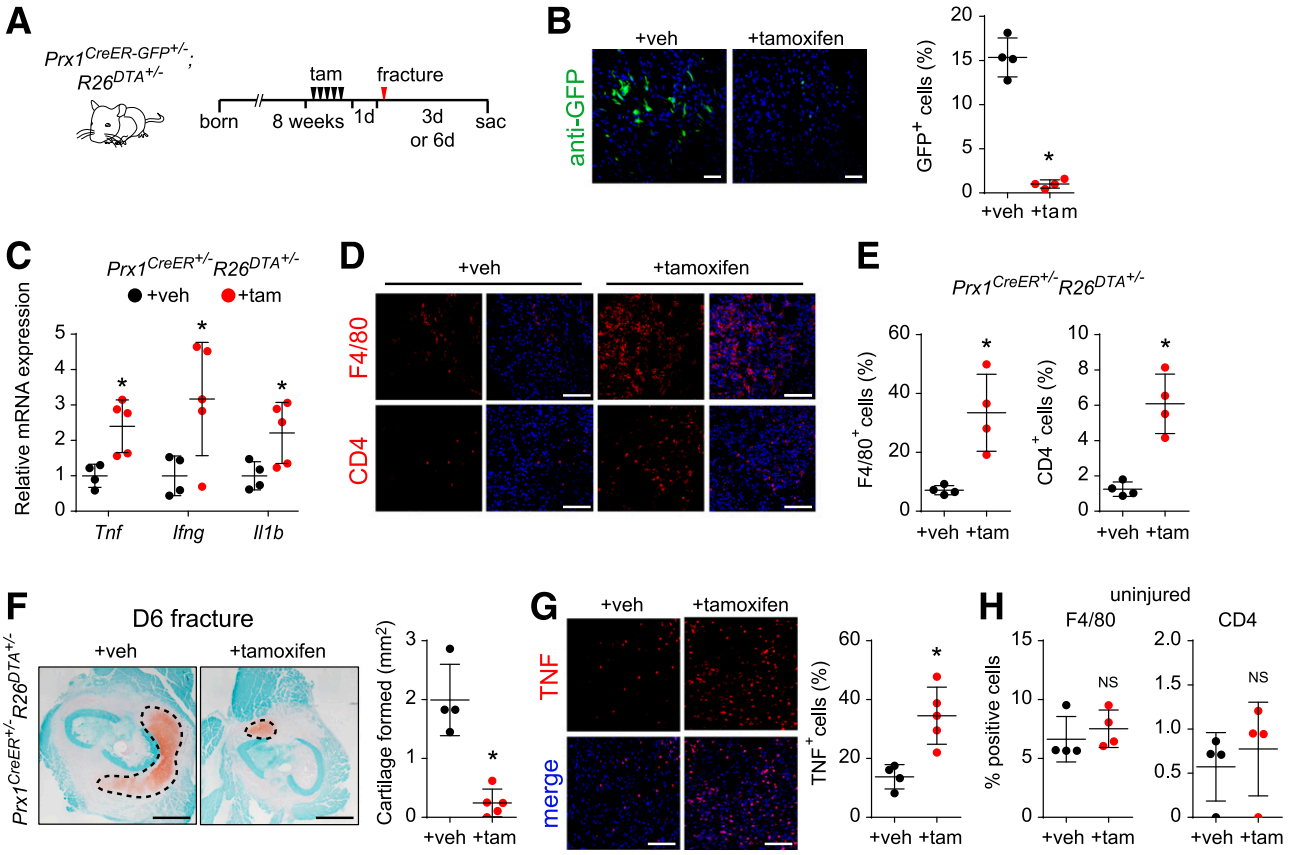

Figure 1—SSC ablation causes prolonged inflammation during fracture healing. *A*: Experimental design for diphtheria toxin–induced ablation of SSCs in experimental (*Prx1*$^{CreER\text{-}GFP+}$*R26*^{DTA}) mice. *B*: Immunofluorescence with GFP antibody to detect Prx1$^+$ cells in day (d) 3 fractures. Quantification of GFP-immunopositive cells in experimental mice that received corn oil (+veh) or tamoxifen (+tam). Scale bars, 50 μm. *C*: mRNA expression of *Tnf*, *Il1b*, and *Ifng* from day 3 fractures of experimental mice that received corn oil or tamoxifen, as determined by RT-qPCR. *D*: Representative immunofluorescent images of F4/80- or CD4-immunopositive cells in day 3 fractures in the control (+veh) or SSC-ablation group (+tam). Scale bars, 100 μm. *E*: Quantification of F4/80- or CD4-immunopositive cells per total nucleated cells in day 3 fractures in experimental mice that received vehicle or tamoxifen. *F*: Representative images of day 6 (D6) fracture wounds from control or SSC ablation group stained with Safranin O/Fast Green (left) and quantification of cartilage formed in area (mm^2) (right). Scale bars, 1 mm. *G*: Representative immunofluorescent images of TNF$^+$ cells in day 6 fracture wounds, analyzed in mesenchymal area between cartilage and muscle compartments (left) and quantification of TNF$^+$ cells in +veh or +tam group (right). Scale bars, 100 μm. *H*: Quantification of F4/80- or CD4-positive cells per total nucleated cells (%) in the periosteal layer of uninjured contralateral femurs. Data are represented as mean ± SD. $N = 4$ to 5 mice each. *$P < 0.05$ comparing corn oil control to tamoxifen groups, two-tailed *t* test. sac, sacrifice.

by inhibiting NF-κB activation in SSCs suggests a pathologic role of NF-κB during diabetic healing. Moreover, inhibition of NF-κB in SSCs had little effect on normoglycemic wounds (Fig. 3*D* and *E*), indicating that there is an aspect to diabetes that induces NF-κB dysregulation that is not present in normoglycemic animals.

We next determined if high glucose could induce NF-κB dysregulation in SSCs by examining BMSSCs, a heterogeneous population of endosteal and stromal cells that represent a subset of SSCs. High glucose significantly increased NF-κB activation in BMSSCs, elevated mRNA levels of *Tnf* and *Il1b*, and greatly reduced *Tgfb1* mRNA levels (Fig. 3*F* and *G*). High glucose–induced changes were blocked in BMSSCs from experimental mice (Fig. 3*G*), consistent with results seen in diabetic animals in vivo. In control experiments, BMSSCs isolated from *Prx1*$^{Cre+}$*Ikkβ*$^{f/f}$ mice had reduced IKKβ protein and mRNA expression when compared with BMSSCs from control mice (Supplementary Fig. 2).

To determine whether NF-κB activation in SSCs had an impact on subsequent healing events, we examined callus size and production of cartilage matrix. Diabetic mice had significantly reduced callus size and cartilage production by 39% and 58%, respectively (Fig. 4*A* and *B*). NF-κB inhibition in SSCs completely rescued the production of callus and cartilage in diabetic fractures (Fig. 4*B*). Of note, lineage tracing of Prx1$^+$ SSCs showed labeled SSCs near the injury site in day 3 fractures but also labeled chondrocytes that derived from SSCs by day 6 (Supplementary Fig. 3), raising the possibility that genetic perturbation in chondrocytes may contribute to the rescued phenotype. To test if chondrocyte-specific NF-κB inhibition reversed the effects of diabetes, we generated *Col2α1*$^{Cre+}$*Ikkβ*$^{f/f}$ mice (28). NF-κB inhibition in chondrocytes

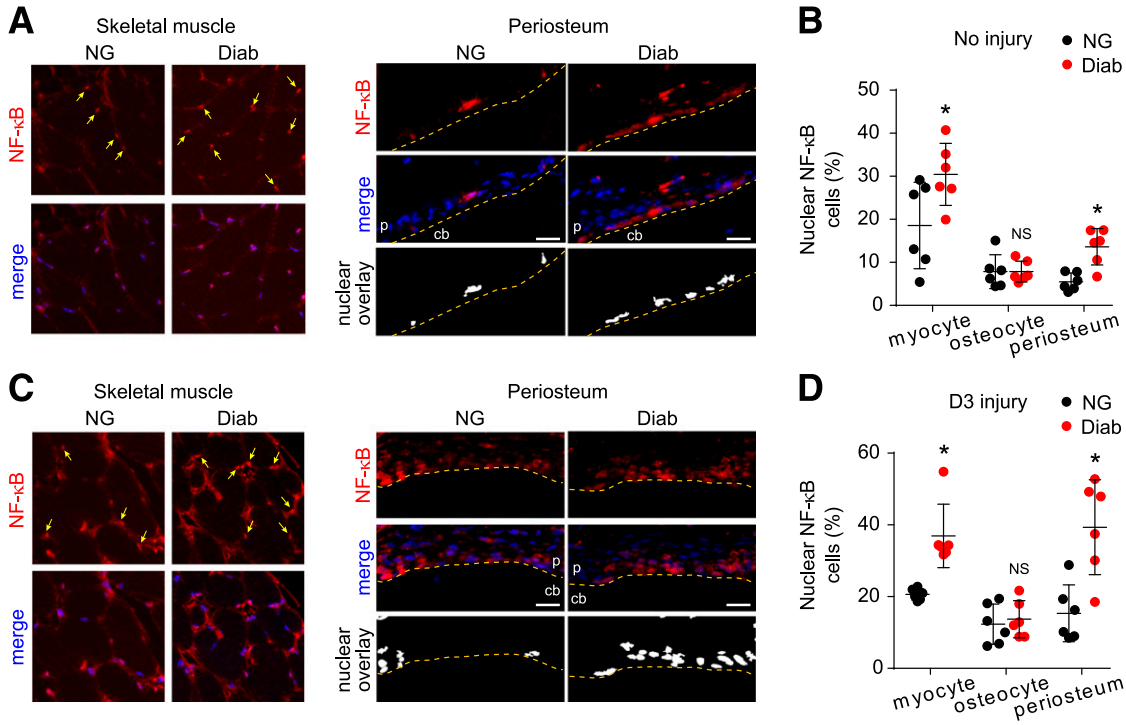

Figure 2—Diabetes enhances NF-κB activation in periosteal cells. *A*: Immunofluorescence of NF-κB (p65) in skeletal muscle and periosteum of uninjured femur. Nuclear NF-κB expression is indicated by yellow arrows (skeletal muscle) or by the nuclear overlay image with DAPI expression (periosteum). Representative images from normoglycemic (NG) and diabetic (Diab) mice are displayed. Scale bars, 20 μm. *B*: Quantification of cells with nuclear NF-κB expression in skeletal muscle (myocyte), cortical bone (osteocyte), and periosteum in an uninjured femur of NG or Diab mice. *C*: Immunofluorescence of NF-κB (p65) in NG or Diab mice that received femoral fracture and healed for 3 days. Representative images are shown. Scale bars, 20 μm. *D*: Quantification of cells with nuclear NF-κB expression in NG or Diab mice that healed for 3 days postfracture (D3 injury). Data are represented as mean ± SD. $N = 6$ mice each group. $^*P < 0.05$ comparing NG to Diab groups. NS, two-tailed *t* test. cb, cortical bone; p, periosteum.

failed to rescue the negative effect of diabetes on callus and cartilage formation (Fig. 4*C* and *D*), ruling out chondrocytes as a potential rescue source. Lastly, we asked whether postnatal SSCs are responsible for preventing the impact of diabetes by generating mice with tamoxifen-inducible NF-κB inhibition ($Prx1^{CreER+}Ikk\beta^{f/f}$). We first confirmed through lineage tracing in $Prx1^{CreER+}R26^{TdTomato}$ mice that postnatal SSCs are labeled by day 3 and expand rapidly throughout day 6 postfracture (Fig. 4*E*). Similar to results with constitutive NF-κB inhibition, conditional tamoxifen-induced NF-κB inhibition in SSCs reversed the reduction in cartilage formation caused by diabetes (Fig. 4*F* and *G*). Thus, by both constitutive and induced blockage of NF-κB activation, we demonstrated that SSCs but not chondrocytes are critical in rescuing the impact of diabetes on the early events of fracture repair.

To examine a downstream effect of dysregulated NF-κB activation in SSCs, we assessed its impact on SSC numbers quantified by immunofluorescence with antibodies specific to SSC markers CD271 and Sca1 (29,30). Diabetes caused a large decrease in $CD271^+$ SSCs on day 3 and 6 fractures compared with normoglycemic mice, and this loss was prevented by NF-κB inhibition (Fig. 5*A* and *B*). Similar results were obtained for $Sca1^+$ SSCs (Fig. 5*A* and *C*). Further experiments demonstrated that diabetes-induced loss of SSCs was also blocked by conditional NF-κB inhibition in postnatal SSCs (Fig. 5*D*). In control experiments, we determined that CD271 and Sca1 colocalized with RFP produced by $Prx1^{Cre+}R26^{TdTomato}$ reporter mice, consistent with Prx1 lineage-specific expression in SSCs (31), whereas SSCs did not express CD45, a hematopoietic cell marker (Supplementary Fig. 4).

The above results demonstrate that diabetes caused the loss of SSCs and linked this decrease to aberrant NF-κB activation in SSCs. We next examined potential mechanisms by examining the impact of NF-κB dysregulation on SSC apoptosis and proliferation. SSC apoptosis was assessed by counting double-positive $CD271^+TUNEL^+$ cells in the healing fractures. Diabetes led to a substantial 86% increase in SSC apoptosis, which was completely blocked by NF-κB inhibition in SSCs (Fig. 5*E*). Mechanistically, this was linked to the effect of high glucose, which mimicked diabetes-induced increase in BMSSC apoptosis in vitro that was reversed by NF-κB inhibition (Fig. 5*F*). Diabetes in vivo and high glucose in vitro also reduced SSC proliferation that was rescued by inhibition of NF-κB, although the magnitude of the effect was less than that of apoptosis (Fig. 5*G* and *H*). To further establish how high glucose modulated SSC apoptosis and proliferation, we examined downstream gene expression. High glucose led

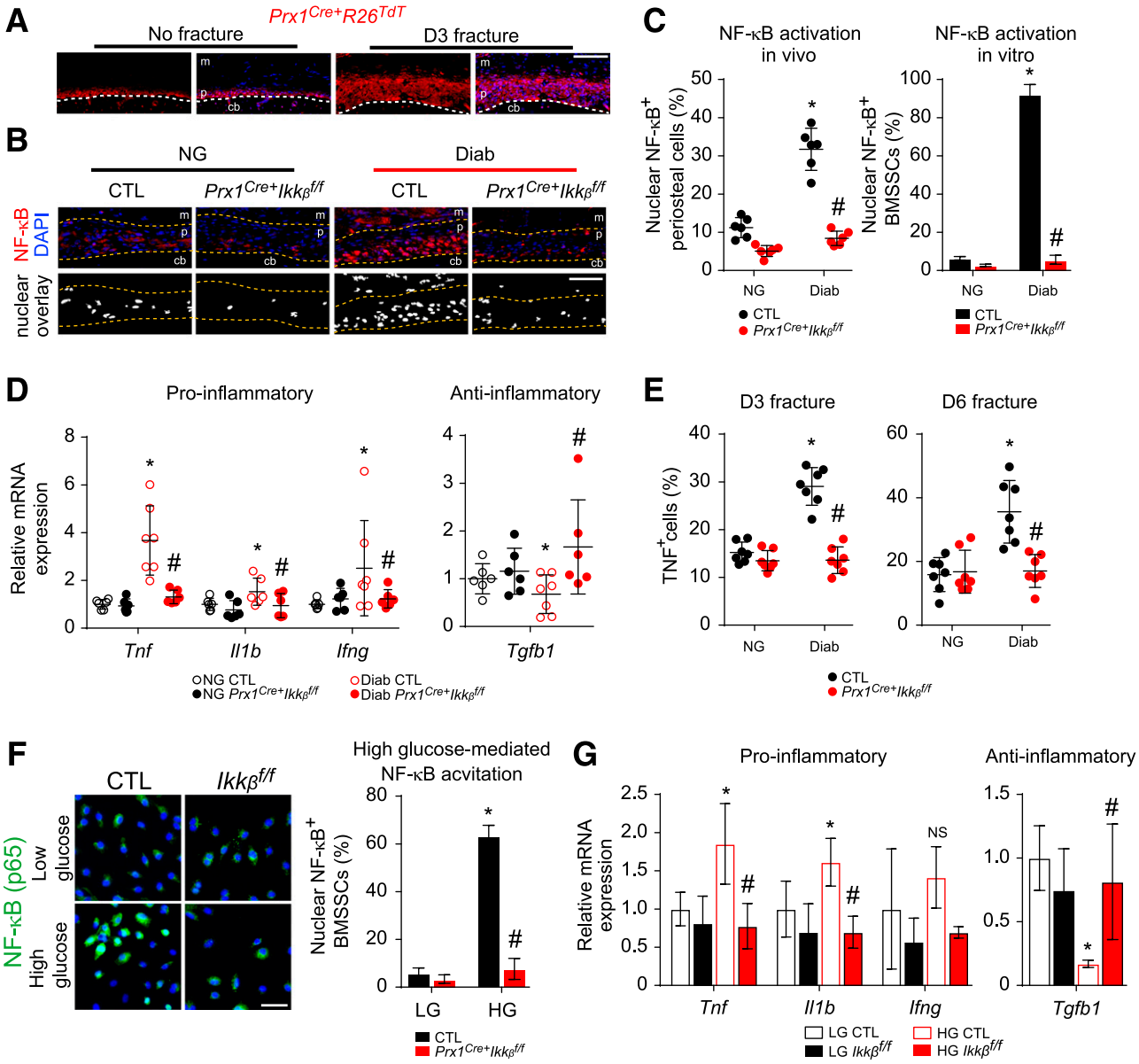

Figure 3—NF-κB inhibition in SSCs prevents diabetes-mediated inflammation. *A*: Lineage tracing in *Prx1*$^{Cre+}$*R26*^{TdTomato} mice. Representative images of periosteum in unfractured femur and 3-day fracture. Scale bar, 100 μm. *B*: Nuclear NF-κB expression by immunofluorescence in periosteum of 3-day fracture from normoglycemic (NG) or diabetic (Diab) control (CTL; *Prx1*$^{Cre-}$*Ikkβ*$^{f/f}$) and experimental (*Prx1*$^{Cre+}$*Ikkβ*$^{f/f}$) mice. NF-κB expression is identified through its overlap with DAPI expression (nuclear overlay). Scale bar, 50 μm. *C*: Quantification of periosteal cells (left) and BMSSCs (right) with nuclear NF-κB expression, per total nucleated cells. *D*: mRNA expression of *Tnf*, *Il1b*, *Ifng*, and *Tgfb1* from day 3 fractures, as determined by RT-qPCR. *E*: TNF^{+} immunopositive cells were counted and quantified by percent of total nucleated cells in day 3 and 6 fractures. *F*: Immunocytochemistry with NF-κB antibody in BMSSC-CM incubated under low-glucose (LG; 4.5 mmol/L) or high-glucose (HG; 25 mmol/L) conditions. Cells immunopositive for nuclear NF-κB were quantified as percent of total cells. Scale bar, 20 μm. *G*: mRNA expression of *Tnf*, *Il1b*, *Ifng*, and *Tgfb1* cytokines in BMSSCs isolated from CTL or experimental mice, as determined by RT-qPCR. Data are represented as mean ± SD. $N = 6$ to 7 each group (*C–E*); three independent experiments from three mice (*F* and *G*). *$P < 0.05$ comparing NG CTL to Diab CTL groups; #$P < 0.05$ comparing Diab CTL to Diab experimental groups; two-way ANOVA with Tukey post hoc test for multigroup comparisons. cb, cortical bone; m, muscle; p, periosteum.

to increased expression of apoptotic genes (*Casp3* and *Casp8*) and cell cycle arrest genes (*P21* and *P27*), which was blocked in BMSSCs that were derived from experimental mice that had lineage-specific NF-κB inhibition (Fig. 5*I*). Thus, diabetes caused a loss of SSCs due to increased apoptosis and, to a lesser effect, reduced proliferation, both of which are mediated by aberrant NF-κB activation that can be induced by high glucose levels.

We next examined how SSCs limit inflammation during healing by examining a downstream cellular event. Given the relatively high number of macrophages (Supplementary Fig. 5), we postulated that SSCs promote

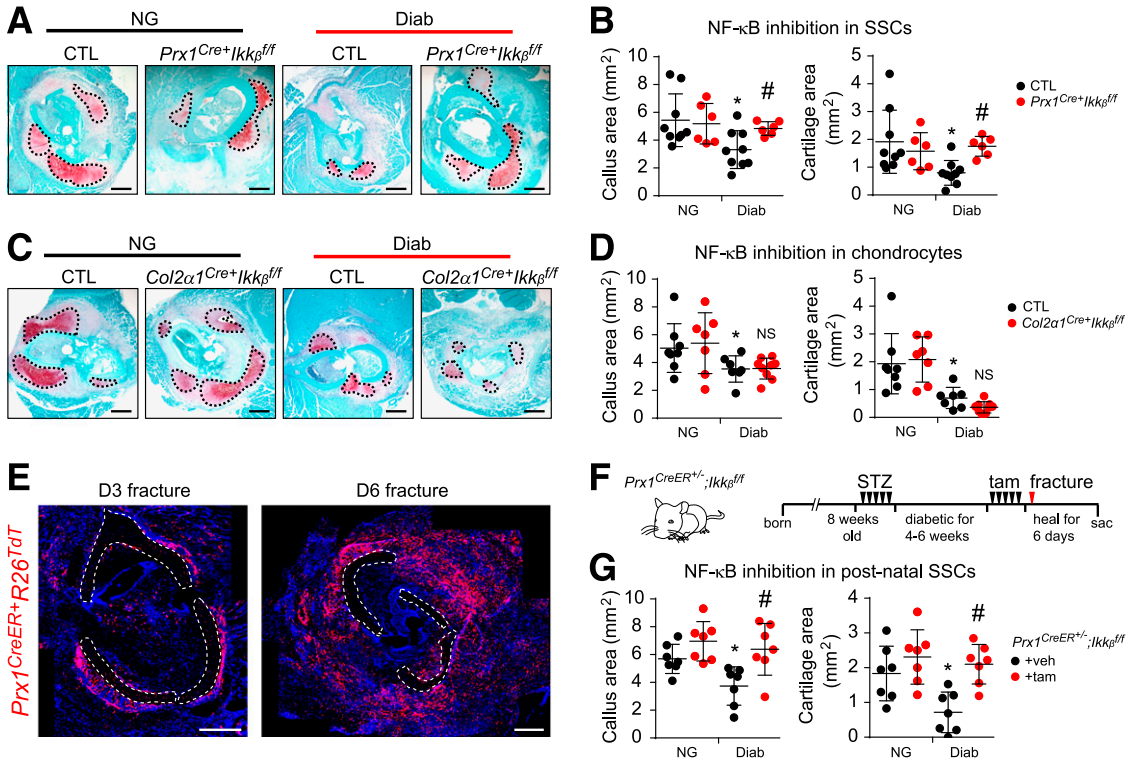

Figure 4—NF-κB inhibition in SSCs but not chondrocytes restores cartilage formation. *A*: Safranin O and Fast Green staining in day 6 fractures of normoglycemic (NG) or diabetic (Diab) control (CTL; $Prx1^{Cre-}Ikk\beta^{f/f}$) and experimental ($Prx1^{Cre+}Ikk\beta^{f/f}$) mice. Representative images are shown. Scale bars, 0.5 mm. *B*: Histomorphometric analysis of callus area (left) and cartilage formation (right) in NG or Diab CTL and experimental mice with NF-κB inhibition in SSCs. *C*: Safranin O and Fast Green staining in day 6 fractures of NG or Diab CTL ($Col2\alpha1^{Cre-}Ikk\beta^{f/f}$) and experimental ($Col2\alpha1^{Cre+}Ikk\beta^{f/f}$) mice. Representative images are shown. Scale bars, 0.5 mm. *D*: Quantification of callus area (left) and cartilage formation (right) in NG or Diab CTL and experimental mice with NF-κB inhibition in chondrocytes. *E*: Lineage tracing in $Prx1^{CreER+}R26^{TdTomato}$ mice that healed for 3 days (left) or 6 days (right) postfracture. Representative stitched images are shown. Scale bars, 0.5 mm. *F*: Schematic diagram of experimental approach for NF-κB inhibition in postnatal SSCs. *G*: Callus and cartilage area quantification in day 6 fractures of $Prx1^{CreER+/-}Ikk\beta^{f/f}$ NG or Diab mice with corn oil (+veh) or tamoxifen (+tam) administration. Data are represented as mean ± SD. $^*P < 0.05$ comparing NG CTL to Diab CTL groups; $\#P < 0.05$ comparing Diab CTL to Diab experimental groups. NS, two-way ANOVA with Tukey post hoc test. $N = 6–9$ each group. sac, sacrifice; tam, tamoxifen; veh, vehicle.

resolution of inflammation by inducing M2 polarization and that diabetes interferes with the capacity of SSCs to regulate polarization due to altered NF-κB regulation. Immunofluorescence was carried out to quantify proinflammatory M1 as $F4/80^+iNOS^+$ cells and proresolving M2 as $F4/80^+CD163^+$ cells (32). Diabetic fractures had a significantly higher M1 count compared with normoglycemic fractures, whereas M2 numbers were drastically reduced (Fig. 6*A* and *B*). Surprisingly, the low level of M2 macrophages and high level of M1 macrophages caused by diabetes were completely rescued by lineage-specific NF-κB inhibition in SSCs. Thus, through NF-κB activation in SSCs, diabetes causes an imbalance in the M1/M2 macrophage ratio that is proinflammatory.

To identify a mechanism through which NF-κB in SSCs affects macrophage polarization, we examined expression of TGF-β1, a cytokine known to modulate M1/M2 balance (23,33). $Prx1^+$ SSCs expressed TGF-β1 during early fracture healing in normoglycemic mice (Fig. 6*C*). Diabetes largely decreased TGF-β1 expression, which was reversed in vivo by lineage-specific NF-κB inhibition (Fig. 6*D*). Incubating BMSSCs in high glucose closely reproduced the effect of diabetes on reducing TGF-β1 protein levels in vitro (Fig. 6*E*). The loss of TGF-β1 was directly linked to NF-κB, as high glucose–inhibited TGF-β1 expression was blocked in BMSSCs obtained from experimental mice with *Ikkβ* deletion. To test this further, we incubated BMMs with BMSSC-CM cultures and low-dose LPS or IL-4 to avoid saturation of M1 and M2 responses, respectively. Under standard conditions, BMSSC-CM had little effect on M1 but stimulated high levels of M2 polarization (Fig. 6*F* and *G*). M1 polarization was significantly increased by BMSSC-CM incubated with high glucose, whereas M2 polarization was inhibited (Fig. 6*F* and *G*). Blocking NF-κB activation in BMSSCs rescued the effect of high glucose on BMSSC-induced macrophage polarization. TGF-β1–neutralizing antibody prevented BMSSC-CM from upregulating M2 polarization under standard conditions (Fig. 6*H*) and prevented M2 polarization induced by BMSSC-CM from experimental

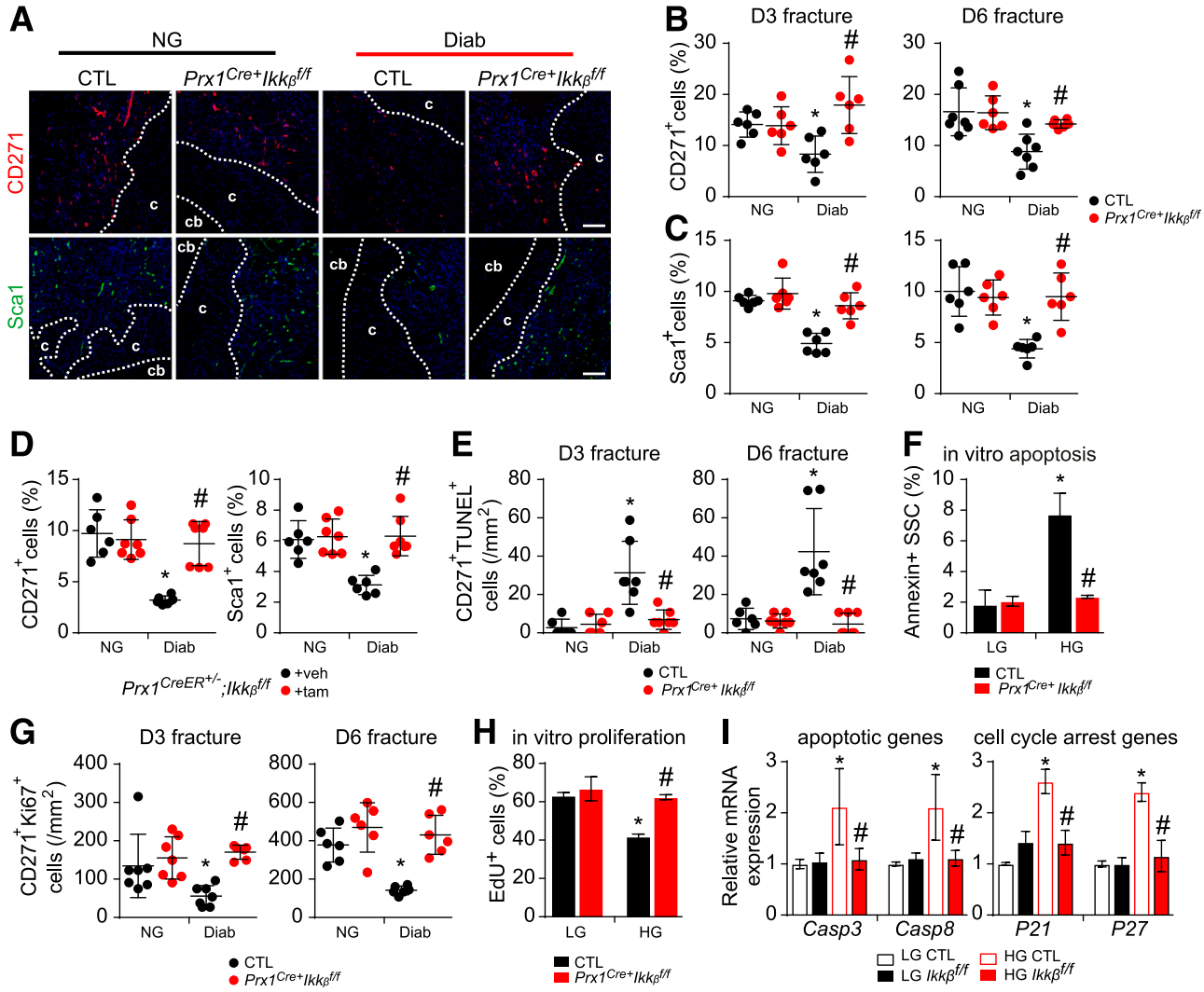

Figure 5—Diabetes reduces SSC numbers by altering apoptosis and proliferation through NF-κB. *A*: Immunofluorescence of CD271 (top) and Sca1 (bottom) in normoglycemic (NG) or diabetic (Diab) control (CTL) and experimental ($Prx1^{Cre+}Ikk\beta^{f/f}$) mice. Representative images are shown, and dashed line demarcates cartilage-mesenchyme border. Scale bars, 100 μm. Quantification of CD271- (*B*) and Sca1-immunopositive (*C*) cells per total nucleated cells in NG or Diab CTL and $Prx1^{Cre+}Ikk\beta^{f/f}$ mice. Data from day 3 (left; D3) and day 6 (right; D6) fractures are shown. *D*: Quantification of CD271- and Sca1-immunopositive cells in $Prx1^{CreER+/-}Ikk\beta^{f/f}$ NG or Diab mice with corn oil (+veh) or tamoxifen (+tam) administration. *E*: Immunofluorescence of CD271 and TUNEL to count double-positive cells (apoptotic SSCs) in D3 and D6 fractures of NG or Diab CTL and $Prx1^{Cre+}Ikk\beta^{f/f}$ mice. *F*: Control or experimental BMSSCs were isolated and incubated in low glucose (LG; 4.5 mmol/L) or high glucose (HG; 25 mmol/L) for 5 days under low-serum conditions, followed by immunocytochemistry with Annexin to detect apoptotic BMSSCs in vitro. Quantification of $Annexin^+$ cells per total nucleated cells. *G*: Immunofluorescence of CD271 and Ki67 to count proliferative SSCs as $CD271^+Ki67^+$ cells. Quantification of double-positive cells in D3 and D6 fractures of NG or Diab CTL and $Prx1^{Cre+}Ikk\beta^{f/f}$ mice. *H*: Serum-induced proliferation of control or experimental BMSSCs after LG or HG incubation for 5 days, quantified by EdU incorporation. EdU^+ cells per total nucleated cells were quantified by immunocytochemistry in vitro. *I*: mRNA expression of apoptotic genes (*Casp3* and *Casp8*) and cell cycle arrest genes (*P21* and *P27*) in control and experimental BMSSCs incubated under LG or HG conditions, as determined by RT-qPCR. Data are represented as mean ± SD. $N = 6$ to 7 mice each group (*B–E* and *G*); three independent experiments from three mice (*F*, *H*, and *I*). *$P < 0.05$ comparing NG CTL to Diab CTL groups; #$P < 0.05$ comparing Diab CTL to Diab experimental groups; two-way ANOVA with Tukey post hoc test for multigroup comparisons. c, cartilage; cb, cortical bone.

BMSSCs in high glucose. These experiments demonstrate that TGF-β1 is a key mediator expressed by SSCs to modulate M2 polarization and that the inability of SSCs to induce M2 polarization through TGF-β1 in high glucose is due to NF-κB activation.

Based on our results above, we speculated that exogenous delivery of TGF-β1 would compensate for the lack of its expression by SSCs and reverse overt inflammation in diabetic fractures. To test this, we administered recombinant TGF-β1 or vehicle in the fracture site of normoglycemic or diabetic mice 24 h postinjury to focus on resolution of inflammation rather than the first inflammatory events (Fig. 7*A*). We found that TGF-β1 administration led to a large reduction of TNF^+ cells in diabetic fractures (Fig. 7*B* and *C*). Consistently, the number of M2 was rescued in diabetic mice that received TGF-β1, returning to normal

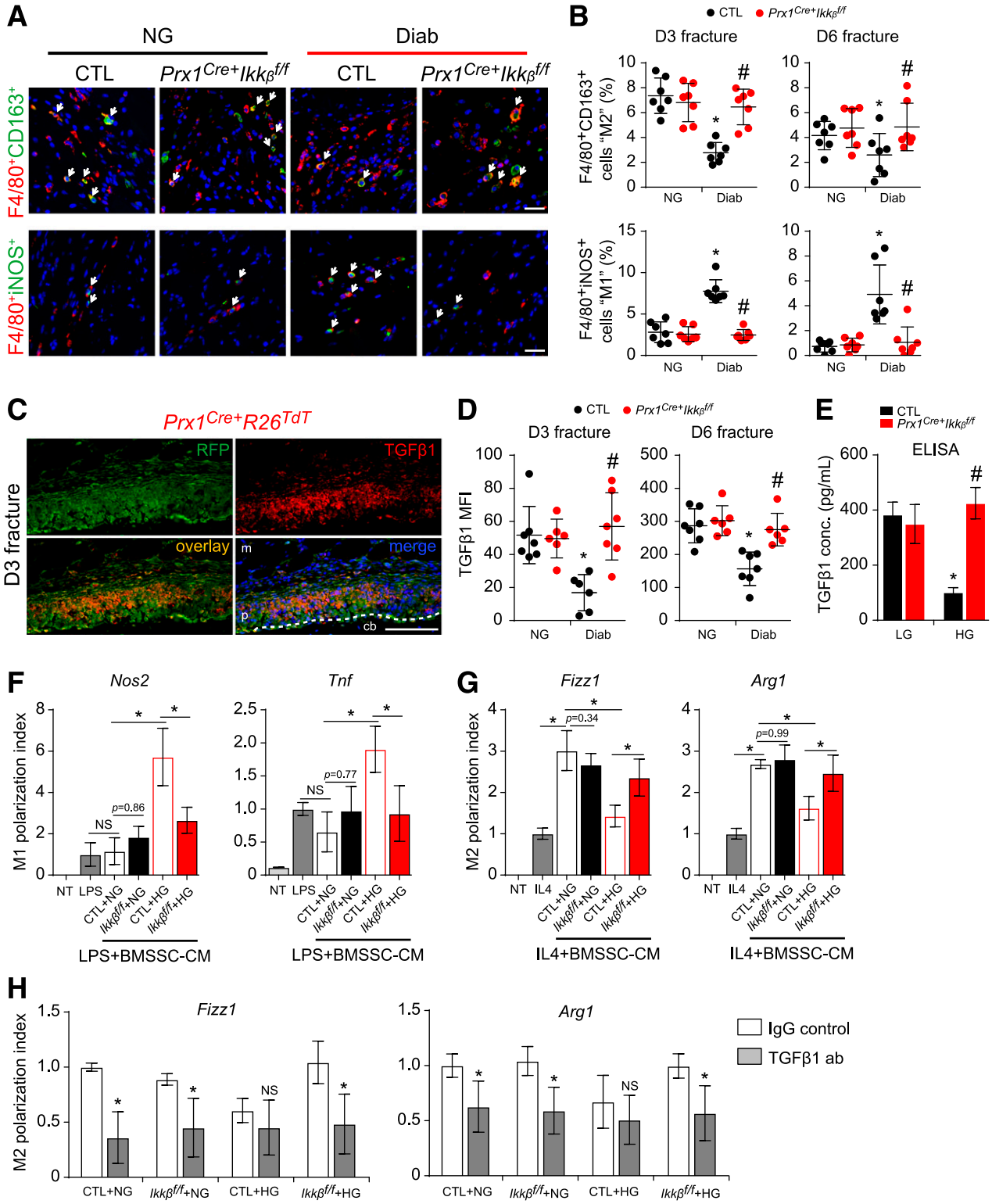

Figure 6—SSCs modulate M1/M2 polarization through TGF-β1 during fracture healing, which is impaired in diabetes by NF-κB activation. *A*: Double immunofluorescence to detect M2 (F4/80$^+$CD163$^+$) and M1 (F4/80$^+$iNOS$^+$) macrophages in normoglycemic (NG) or diabetic (Diab) control (CTL; *Prx1*$^{Cre-}$*Ikkβ*$^{f/f}$) or experimental (*Prx1*$^{Cre+}$*Ikkβ*$^{f/f}$) mice. Representative images show white arrows pointing to M2 in day 3 (D3) fractures and M1 in day 6 (D6) fractures. Scale bars, 50 μm. *B*: Quantification of M2- and M1-immunopositive cells per total nucleated cells in D3 and D6 fractures, as determined by immunofluorescence. *C*: Immunofluorescence with RFP (detection with Alexa 488) and TGF-β1 (detection with Cy5) antibody in D3 fracture periosteum from *Prx1*^{Cre};*R26*^{TdTomato} mice. Scale bar, 100 μm. *D*: TGF-β1 expression as determined by immunofluorescence with TGF-β1 antibody in day 3 and day 6 fracture of NG or Diab control or experimental mice. Data are expressed as MFI. *E*: TGF-β1 concentration in BMSSC-CM from control or experimental mice, incubated in low-glucose (LG) or high-glucose (HG) conditions, as determined by ELISA. *F*: M1 polarization index from BMMs stimulated with LPS and BMSSC-CM from control or experimental BMSSCs with LG or HG incubation, as determined by RT-qPCR for *Nos2* and *Tnf*. Data are normalized to LPS alone (10 ng/mL).

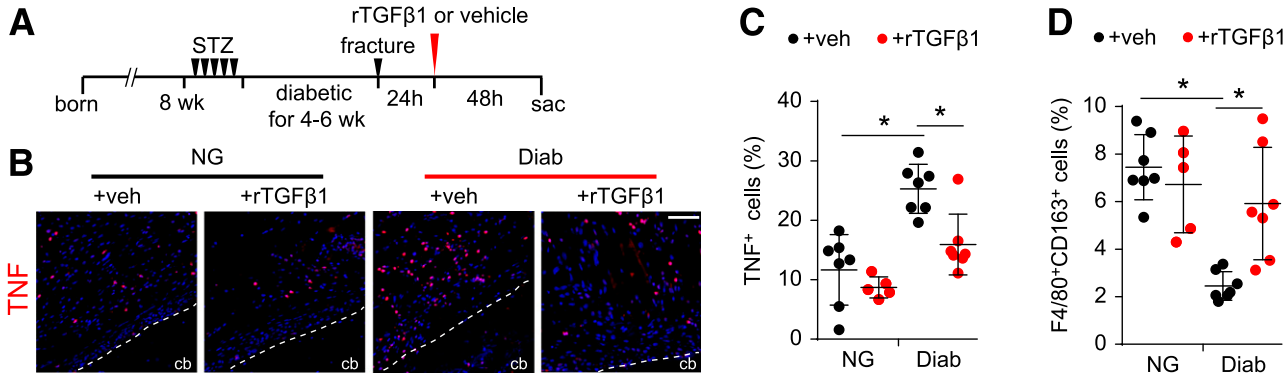

Figure 7—TGF-β1 treatment improves inflammation in diabetic fractures. *A*: Experimental approach for TGF-β1 treatment. *B*: Immunofluorescence with TNF antibody in normoglycemic (NG) or diabetic (Diab) mice that received PBS only (+veh) or recombinant TGF-β1 (+rTGFβ1). Dashed line demarcates cortical bone (cb). Scale bar, 100 μm. *C*: Quantification of TNF^+ cells per total nucleated cells in day 3 fractures of NG or Diab mice that received PBS or rTGF-β1. *D*: Quantification of M2 ($F4/80^+CD163^+$ immunopositive cells) per total nucleated cells in day 3 fractures. Data are represented as mean ± SD. *$P < 0.05$; two-way ANOVA with Tukey post hoc test. $N = 5$–7 each group. sac, sacrifice; STZ, streptozotocin.

levels (Fig. 7*D*). Therefore, TGF-β1 treatment substantially reversed diabetes-mediated dysregulation of M2 polarization and inflammation.

DISCUSSION

The underlying cause for a failure to resolve elevated inflammation in diabetic wounds is poorly understood. In this study, we report that endogenous SSCs play a pivotal role in downregulating inflammation during the early healing process of osseous wounds and that diabetes interferes with this resolution specifically through aberrant NF-κB activation in SSCs. Specific ablation of SSCs in healing fractures led to persistent inflammation, suggesting a critical link between proper SSC expansion and resolution of inflammation. Surprisingly, diabetes affected fracture healing through a reduction of SSCs and enhanced inflammation, both of which were caused by hyperactivation of NF-κB. Lineage-specific inhibition of NF-κB in SSCs through *Ikkβ* deletion reversed diabetes-enhanced apoptosis and reduced proliferation of SSCs, thus preventing the loss of SSCs and restoring tissue regeneration. Aberrant NF-κB activation also impaired the ability of SSCs to express TGF-β1 and induce the formation of M2 macrophages, which was rescued in experimental animals. In diabetic animals, macrophage polarization favored proinflammatory M1 over proresolving M2 polarization in vivo. The negative impact of diabetes was reversed by increasing TGF-β1 either by restoring SSC-produced TGF-β1 through inhibition of NF-κB or by administration of recombinant TGF-β1. Taken together, our findings provide definitive evidence that diabetes leads to NF-κB dysregulation in endogenous SSCs, which is a central pathologic factor in disrupting the early repair process.

In vivo evidence demonstrating a role of SSCs on modulating inflammation has been limited because of relatively low abundance of SSCs under homeostatic conditions. Using a fracture-healing model in which SSCs expand, and with genetic tools to selectively ablate them, we demonstrated that the loss of SSCs was a key factor that causes the failure to resolve inflammation indicated by the high TNF levels. Persistent TNF signaling is detrimental for proper tissue regeneration and homeostasis in most organs through its impact on stem cell proliferation (34–36). In particular, high levels of TNF are characteristic of diabetic fracture healing (4,37,38), and specific inhibition of TNF can partly restore bone formation (39). Given the negative impact of unresolved TNF levels on stem cells, its dysregulation by impaired SSC function may trigger a pathologic positive-feedback loop to further compromise the expansion of SSCs, consequently attributing to delayed tissue regeneration.

We investigated a potential role of NF-κB during diabetic osseous healing and discovered that it had a detrimental effect on SSC expansion by promoting apoptosis and inhibiting proliferation. Although NF-κB typically has a direct antiapoptotic effect (40), it has been reported to promote apoptosis and inhibit proliferation under diabetic conditions (41,42). This polarizing role of NF-κB may be

G: M2 polarization index from BMMs stimulated with IL-4 with or without BMSSC-CM, as determined by RT-qPCR for *Fizz1* and *Arg1*. Data are normalized to IL-4 alone (1.25 ng/mL). *H*: M2 polarization index from BMMs incubated in BMSSC-CM with IL-4 plus TGF-β1–neutralizing antibody (ab) or control IgG, as determined by RT-qPCR for *Fizz1* and *Arg1*. Data are normalized to BMSSC-CM IgG control group. Data are represented as mean ± SD. Student *t* test for *G*. $N = 6$ to 7 each group (*A*–*C*); three independent experiments from three mice (*D*–*G*). *$P < 0.05$ comparing NG CTL to Diab CTL; #$P < 0.05$ comparing Diab CTL to Diab experimental mice; two-way ANOVA with Tukey post hoc test. cb, cortical bone; conc., concentration; m, muscle; NT, not treated; p, periosteum.

explained by its diverse cross talk with other signaling pathways (43) and/or an epigenetic signature that is modified by persistent hyperglycemia (44). We also found that NF-κB dysregulation in SSCs interfered with resolution of inflammation in diabetic fractures, similar to that seen with selective SSC ablation. Thus, maintaining SSC numbers during fracture healing is critical for limiting inflammation, and in diabetic fractures, this process is interrupted through aberrant NF-κB activation in SSCs. Our results also provide an explanation for why diabetes decreases the efficacy of transplanted SSCs to enhance hard and soft tissue repair (45,46) by suggesting that a diabetic environment is unfavorable for normal SSC function. Interestingly, NF-κB inhibition in SSCs had minimal effects in normoglycemic wounds, likely due to relatively little NF-κB activation in SSCs in normal compared with those in diabetic wounds (Fig. 3*B* and *C*).

The second major effect of diabetes on fracture wounds was the impairment of macrophage transition from M1 to M2, which was rescued when NF-κB was blocked in SSCs. This finding indicates that SSCs are responsible for the proper M1/M2 balance during osseous healing and are disrupted under diabetic conditions. SSC dysregulation through NF-κB is likely to contribute to other types of diabetic wounds in which persistent inflammation and predominance of M1 over M2 is observed (47,48). Mechanistically, this was due to NF-κB–mediated reduction of TGF-β1 expression by SSCs caused by diabetes in vivo and by high glucose in vitro. BMSSC-CM culture stimulated M2 polarization, which was blocked by glucose-induced NF-κB activation that was directly related to a failure to express TGF-β1. In humans, early fracture healing coincides with an increase in TGF-β1 serum concentration levels, whereas subjects who experience difficulty in healing, such as formation of nonunions, exhibit significantly lower TGF-β1 levels (25,49). While our findings clearly demonstrate M1/M2 imbalance in diabetic fracture wounds and suggest modulation of phenotype switching by TGF-β1 as a mechanism, we cannot rule out other potential cellular events such as differential recruitment of M1 or M2 egression. Moreover, our results suggest that the formation of M2, which occurs in normoglycemic but not diabetic wounds, is important in resolving inflammation in early fracture repair. The important role of TGF-β1 in modulating inflammation and promoting skeletal regeneration is further supported by the findings that diabetic inflammation was largely reduced along with the recovery of M2 when recombinant TGF-β1 was administered during early fracture healing. Thus, suppression of TGF-β1 signaling is a key mechanism by which diabetes-enhanced NF-κB activation limits the capacity of SSCs to resolve inflammation in diabetic fracture wounds.

In summary, our study unveils a mechanism by which T1D impairs endogenous SSCs to enhance inflammation and impair healing response, in which aberrant activation of NF-κB plays a key role. The deficit in SSC function due to NF-κB dysregulation can be linked to the loss of SSC numbers as well as reduced capacity of SSCs to produce TGF-β1 that modulates macrophage polarization. Although our study used a T1D model, the findings may be applicable to impaired skeletal healing in type 2 diabetes, as downstream activation of NF-κB has been implicated in type 2 diabetes complications in other cell types (19). Furthermore, these results also point to disruption of a critical pathway in SSCs caused by diabetes and may represent a general mechanism for diabetic complications in which stem cells and inflammation play a role in the response to perturbation.

Acknowledgments. The authors thank Dr. Songtao Shi (University of Pennsylvania, Philadelphia, PA) for helpful suggestions and Drs. Patrick O'Connor (Rutgers University, Newark, NJ) and Michael Karin (University of California San Diego, La Jolla, CA) for providing transgenic mice.

Funding. This research was funded by National Institutes of Health grants K08-DE027129 (to K.I.K.) and R01-AR060055 and R01-DE019108 (to D.T.G.). C.C. is supported by National Institute of Dental and Craniofacial Research grant K99/R00-DE025915.

Duality of Interest. No potential conflicts of interest relevant to this article were reported.

Author Contributions. K.I.K., A.L.S., R.M.K., J.C., and B.P.D. performed the experiments and analyzed the data. C.C. provided significant assistance for the cell culture experiments. K.I.K. and D.T.G. designed the experiments, analyzed the data, and wrote the manuscript. D.T.G. conceived the study. D.T.G. is the guarantor of this work and, as such, had full access to all of the data in the study and takes responsibility for the integrity of the data and the accuracy of the data analysis.

Prior Presentation. This study was presented at the 97th General Session of the International Association for Dental Research, Vancouver, British Columbia, Canada, 19–22 June 2019.

References

1. Sellmeyer DE, Civitelli R, Hofbauer LC, Khosla S, Lecka-Czernik B, Schwartz AV. Skeletal metabolism, fracture risk, and fracture outcomes in type 1 and type 2 diabetes. Diabetes 2016;65:1757–1766

2. Weber DR, Schwartz G. Epidemiology of skeletal health in type 1 diabetes. Curr Osteoporos Rep 2016;14:327–336

3. Xu F, Zhang C, Graves DT. Abnormal cell responses and role of TNF-α in impaired diabetic wound healing. BioMed Res Int 2013;2013:754802

4. Alblowi J, Kayal RA, Siqueira M, et al. High levels of tumor necrosis factor-alpha contribute to accelerated loss of cartilage in diabetic fracture healing. Am J Pathol 2009;175:1574–1585

5. Pacios S, Xiao W, Mattos M, et al. Osteoblast lineage cells play an essential role in periodontal bone loss through activation of nuclear factor-kappa B. Sci Rep 2015;5:16694

6. Mirza RE, Fang MM, Ennis WJ, Koh TJ. Blocking interleukin-1β induces a healing-associated wound macrophage phenotype and improves healing in type 2 diabetes. Diabetes 2013;62:2579–2587

7. Fullerton JN, Gilroy DW. Resolution of inflammation: a new therapeutic frontier. Nat Rev Drug Discov 2016;15:551–567

8. Perdiguero E, Sousa-Victor P, Ruiz-Bonilla V, et al. p38/MKP-1-regulated AKT coordinates macrophage transitions and resolution of inflammation during tissue repair. J Cell Biol 2011;195:307–322

9. Chow A, Lucas D, Hidalgo A, et al. Bone marrow CD169+ macrophages promote the retention of hematopoietic stem and progenitor cells in the mesenchymal stem cell niche. J Exp Med 2011;208:261–271

10. Sehgal A, Donaldson DS, Pridans C, Sauter KA, Hume DA, Mabbott NA. The role of CSF1R-dependent macrophages in control of the intestinal stem-cell niche. Nat Commun 2018;9:1272
11. Arnold L, Henry A, Poron F, et al. Inflammatory monocytes recruited after skeletal muscle injury switch into antiinflammatory macrophages to support myogenesis. J Exp Med 2007;204:1057–1069
12. Colnot C. Skeletal cell fate decisions within periosteum and bone marrow during bone regeneration. J Bone Miner Res 2009;24:274–282
13. Einhorn TA, Gerstenfeld LC. Fracture healing: mechanisms and interventions. Nat Rev Rheumatol 2015;11:45–54
14. Chen C, Wang D, Moshaverinia A, et al. Mesenchymal stem cell transplantation in tight-skin mice identifies miR-151-5p as a therapeutic target for systemic sclerosis. Cell Res 2017;27:559–577
15. Liang J, Zhang H, Hua B, et al. Allogenic mesenchymal stem cells transplantation in refractory systemic lupus erythematosus: a pilot clinical study. Ann Rheum Dis 2010;69:1423–1429
16. Pahl HL. Activators and target genes of Rel/NF-kappaB transcription factors. Oncogene 1999;18:6853–6866
17. Wada J, Makino H. Inflammation and the pathogenesis of diabetic nephropathy. Clin Sci (Lond) 2013;124:139–152
18. Ganesh Yerra V, Negi G, Sharma SS, Kumar A. Potential therapeutic effects of the simultaneous targeting of the Nrf2 and NF-κB pathways in diabetic neuropathy. Redox Biol 2013;1:394–397
19. Suryavanshi SV, Kulkarni YA. NF-κβ: a potential target in the management of vascular complications of diabetes. Front Pharmacol 2017;8:798
20. Giacco F, Brownlee M. Oxidative stress and diabetic complications. Circ Res 2010;107:1058–1070
21. Kassan M, Choi SK, Galán M, et al. Enhanced NF-κB activity impairs vascular function through PARP-1-, SP-1-, and COX-2-dependent mechanisms in type 2 diabetes. Diabetes 2013;62:2078–2087
22. Alblowi J, Tian C, Siqueira MF, et al. Chemokine expression is upregulated in chondrocytes in diabetic fracture healing. Bone 2013;53:294–300
23. Zhang F, Wang H, Wang X, et al. TGF-β induces M2-like macrophage polarization via SNAIL-mediated suppression of a pro-inflammatory phenotype. Oncotarget 2016;7:52294–52306
24. Logan M, Martin JF, Nagy A, Lobe C, Olson EN, Tabin CJ. Expression of Cre Recombinase in the developing mouse limb bud driven by a Prxl enhancer. Genesis 2002;33:77–80
25. Jiao H, Xiao E, Graves DT. Diabetes and its effect on bone and fracture healing. Curr Osteoporos Rep 2015;13:327–335
26. Kawanami A, Matsushita T, Chan YY, Murakami S. Mice expressing GFP and CreER in osteochondro progenitor cells in the periosteum. Biochem Biophys Res Commun 2009;386:477–482
27. Li ZW, Omori SA, Labuda T, Karin M, Rickert RC. IKK beta is required for peripheral B cell survival and proliferation. J Immunol 2003;170:4630–4637
28. Ovchinnikov DA, Deng JM, Ogunrinu G, Behringer RR. Col2a1-directed expression of Cre recombinase in differentiating chondrocytes in transgenic mice. Genesis 2000;26:145–146
29. Xiao J, Yang X, Jing W, et al. Adipogenic and osteogenic differentiation of Lin(-)CD271(+)Sca-1(+) adipose-derived stem cells. Mol Cell Biochem 2013;377:107–119
30. Alvarez R, Lee HL, Hong C, Wang CY. Single CD271 marker isolates mesenchymal stem cells from human dental pulp. Int J Oral Sci 2015;7:205–212
31. Duchamp de Lageneste O, Julien A, Abou-Khalil R, et al. Periosteum contains skeletal stem cells with high bone regenerative potential controlled by Periostin. Nat Commun 2018;9:773
32. Edin S, Wikberg ML, Dahlin AM, et al. The distribution of macrophages with a M1 or M2 phenotype in relation to prognosis and the molecular characteristics of colorectal cancer. PLoS One 2012;7:e47045
33. Gong D, Shi W, Yi SJ, Chen H, Groffen J, Heisterkamp N. TGFβ signaling plays a critical role in promoting alternative macrophage activation. BMC Immunol 2012;13:31
34. Baker RG, Hayden MS, Ghosh S. NF-κB, inflammation, and metabolic disease. Cell Metab 2011;13:11–22
35. Zhou Y, Jiang X, Gu P, Chen W, Zeng X, Gao X. Gsdma3 mutation causes bulge stem cell depletion and alopecia mediated by skin inflammation. Am J Pathol 2012;180:763–774
36. Palacios D, Mozzetta C, Consalvi S, et al. TNF/p38α/polycomb signaling to Pax7 locus in satellite cells links inflammation to the epigenetic control of muscle regeneration. Cell Stem Cell 2010;7:455–469
37. Kayal RA, Siqueira M, Alblowi J, et al. TNF-alpha mediates diabetes-enhanced chondrocyte apoptosis during fracture healing and stimulates chondrocyte apoptosis through FOXO1. J Bone Miner Res 2010;25:1604–1615
38. Tevlin R, Seo EY, Marecic O, et al. Pharmacological rescue of diabetic skeletal stem cell niches. Sci Transl Med 2017;9:eaag2809
39. Ko KI, Coimbra LS, Tian C, et al. Diabetes reduces mesenchymal stem cells in fracture healing through a TNFα-mediated mechanism. Diabetologia 2015;58:633–642
40. Hoesel B, Schmid JA. The complexity of NF-κB signaling in inflammation and cancer. Mol Cancer 2013;12:86
41. Tsai KH, Wang WJ, Lin CW, et al. NADPH oxidase-derived superoxide anion-induced apoptosis is mediated via the JNK-dependent activation of NF-κB in cardiomyocytes exposed to high glucose. J Cell Physiol 2012;227:1347–1357
42. Kato H, Taguchi Y, Tominaga K, et al. High glucose concentrations suppress the proliferation of human periodontal ligament stem cells and their differentiation into osteoblasts. J Periodontol 2016;87:e44–e51
43. Oeckinghaus A, Hayden MS, Ghosh S. Crosstalk in NF-κB signaling pathways. Nat Immunol 2011;12:695–708
44. El-Osta A, Brasacchio D, Yao D, et al. Transient high glucose causes persistent epigenetic changes and altered gene expression during subsequent normoglycemia. J Exp Med 2008;205:2409–2417
45. Sui BD, Hu CH, Zheng CX, et al. Recipient glycemic micro-environments govern therapeutic effects of mesenchymal stem cell infusion on osteopenia. Theranostics 2017;7:1225–1244
46. van de Vyver M. Intrinsic mesenchymal stem cell dysfunction in diabetes mellitus: implications for autologous cell therapy. Stem Cells Dev 2017;26:1042–1053
47. Finley PJ, DeClue CE, Sell SA, DeBartolo JM, Shornick LP. Diabetic wounds exhibit decreased Ym1 and arginase expression with increased expression of IL-17 and IL-20. Adv Wound Care (New Rochelle) 2016;5:486–494
48. Bannon P, Wood S, Restivo T, Campbell L, Hardman MJ, Mace KA. Diabetes induces stable intrinsic changes to myeloid cells that contribute to chronic inflammation during wound healing in mice. Dis Model Mech 2013;6:1434–1447
49. Zimmermann G, Henle P, Küsswetter M, et al. TGF-beta1 as a marker of delayed fracture healing. Bone 2005;36:779–785